General Disclaimer

One or more of the Following Statements may affect this Document

- This document has been reproduced from the best copy furnished by the organizational source. It is being released in the interest of making available as much information as possible.

- This document may contain data, which exceeds the sheet parameters. It was furnished in this condition by the organizational source and is the best copy available.

- This document may contain tone-on-tone or color graphs, charts and/or pictures, which have been reproduced in black and white.

- This document is paginated as submitted by the original source.

- Portions of this document are not fully legible due to the historical nature of some of the material. However, it is the best reproduction available from the original submission.

Produced by the NASA Center for Aerospace Information (CASI)

NASA CR-134844

(NASA-CR-134844) CHARGE-EXCHANGE PLASMA GENERATED BY AN ION THRUSTER Annual Report, 1 Jul. 1974 - 30 Jun. 1975 (Colorado State Univ.) 44 p HC $4.25 CSCL 21C G3/20

N75-29172 Unclas 31992

CHARGE-EXCHANGE PLASMA GENERATED BY AN ION THRUSTER

PREPARED FOR

LEWIS RESEARCH CENTER

NATIONAL AERONAUTICS AND SPACE ADMINISTRATION

GRANT NSG 3038

Annual Report

June 1975

Harold R. Kaufman

Department of Physics

Colorado State University

Fort Collins, Colorado

1. Report No.	2. Government Accession No.	3. Recipient's Catalog No.
NASA CR-134844		

4. Title and Subtitle	5. Report Date
"Charge-Exchange Plasma Generated by an Ion Thruster"	June 1975
	6. Performing Organization Code

7. Author(s)	8. Performing Organization Report No.
Harold R. Kaufman	
	10. Work Unit No.

9. Performing Organization Name and Address	11. Contract or Grant No.
Department of Physics Colorado State University Fort Collins, Colorado 80523	NSG 3038
	13. Type of Report and Period Covered Contractor Report July 1, 1974-June 30, 1975

12. Sponsoring Agency Name and Address	14. Sponsoring Agency Code
National Aeronautics and Space Administration Washington, D. C. 20546	

15. Supplementary Notes: Grant Manager, Stanley Domitz
Spacecraft Technology Division
NASA Lewis Research Center
Cleveland, OH 44135

16. Abstract

The use of high-voltage solar arrays can greatly reduce or eliminate power processing requirements in space electric-propulsion systems. But this use also requires substantial areas of solar array to be at high positive potential relative to space and most of the spacecraft. The charge-exchange plasma can conduct electrons from the ion beam to such positive surfaces, and thereby electrically load the high-voltage solar array. To evaluate this problem, the charge-exchange plasma generated by an ion beam has been investigated experimentally. Based upon the experimental data, a simple model was derived for the charge-exchange plasma. This model is conservative in the sense that both the electron/ion density and the electron current density should be equal to, or less than, the predicted value for all directions in the hemisphere upstream of the ion beam direction. Increasing the distance between a positive-potential surface (such as a high-voltage solar array) and the thruster is the simplest way to control interactions. Both densities and currents will vary as the inverse square of this distance.

17. Key Words (Suggested by Author(s))	18. Distribution Statement
Electrostatic Thruster	Unclassified - Unlimited

19. Security Classif. (of this report)	20. Security Classif. (of this page)	21. No. of Pages	22. Price*
Unclassified	Unclassified		$3.00

* For sale by the National Technical Information Service, Springfield, Virginia 22151

TABLE OF CONTENTS

INTRODUCTION

The use of high-voltage solar arrays can greatly reduce or eliminate power processing requirements in space electric-propulsion systems. The positive high voltage used to accelerate beam ions and the low voltage used for the main discharge are most promising for direct use of solar-array power - because these two uses represent the largest blocks of power in an ion thruster. But both of these uses also require substantial areas of solar array to be at a high positive potential relative to space and most of the spacecraft. Such positive potential surfaces, if left exposed, can draw excessive electron currents under some conditions.

Electron currents to positive surfaces involve both the ion beam plasma (the immediate source of the electrons) and the region between the positive surface and the ion beam. The electron density within the ion beam obeys the "barometric" equation,

$$n_e = n_{e,ref} \, \mathrm{Exp}[-qV/kT_e] \, , \qquad (1)$$

which was introduced by Sellen, et al.[1] and verified by Ogawa, et al.[2,3] The potential V is defined as zero at the reference electron density $n_{e,ref}$. Ogawa, et al. found the electron temperature within the ion beam is, in electron volts, equal to about 0.3 of the injection (or coupling) voltage.

The transport of electrons from the ion beam to a positive solar array surface has been treated by Knauer, et al. as an electron space-charge-flow problem.[4] Measured electron currents are higher than calculated by Knauer, et al., however, and are due to conduction in the charge-exchange ion plasma generated by the ion beam.

Charge-exchange ions are produced when fast beam ions pass near the relatively slow escaping neutrals. This process results in fast neutrals (which rapidly escape) and slow ions. Being slow, the charge-exchange ions are affected by small electric fields within the ion beam. In leaving the ion beam, the charge-exchange ions (with some escaping electrons) form the surrounding charge-exchange plasma. Some detailed trajectories of charge-exchange ions have been examined by Komatsu, et al.[5] The overall production rate of charge-exchange ions within the ion beam is also of interest in this investigation and was initially calculated by Staggs, et al.[6] The capability of the charge-exchange plasma to transport electrons to a positive surface was experimentally evaluated by Worlcck, et al.[7] An attempt was made to prevent charge-exchange ions from reaching and coating sensitive surfaces of the ATS-6 spacecraft by biasing the spacecraft +15 volts relative to the thruster neutralizer. This bias resulted in substantial electron currents to the spacecraft.

The study reported herein is an experimental investigation of the charge-exchange plasma surrounding a thruster ion beam. A simple theoretical model is also presented for the generation and propagation of this plasma. The electron currents conducted to positive surfaces by this plasma are also included in this model. SI (mks) units are used throughout.

APPARATUS AND PROCEDURE

Facility and Thruster

The vacuum facility used was the 1.2-m diameter, 4.6-m long chamber at the Engineering Research Center of Colorado State University. An 0.8-m diffusion pump maintained a typical operating pressure of 5×10^{-6} torr while operating. The use of a liquid-nitrogen cooled liner helped maintain this pressure by condensing the mercury propellant.

The thruster was a 15-cm SERT-II design, except for the use of dished grids that permitted higher beam currents than the original flat grids. The positioning of the thruster in the vacuum facility, together with the positioning of the target and the simulated solar array (when used), is indicated in Fig. 1. Normal operation of thrusters in this vacuum facility involves insertion through a vacuum valve, with removal and servicing of the thruster usually possible without exposing the main vacuum chamber to atmospheric pressure. The instrumentation used in this investigation, however, necessitated the opening of the main chamber for any servicing of the thruster. The screen and accelerator potentials were maintained at +1000 and -500 volts throughout the investigation.

Instrumentation

The simulated solar array is shown in Fig. 2. The current collection areas were insulated from each other and the remainder of the array. With electron temperature known from other probe surveys, the currents to these areas could be used to calculate electron/ion density. The simulated array was also insulated from the vacuum facility so that current to the entire surface could be monitored. The geometry of the simulated solar array was

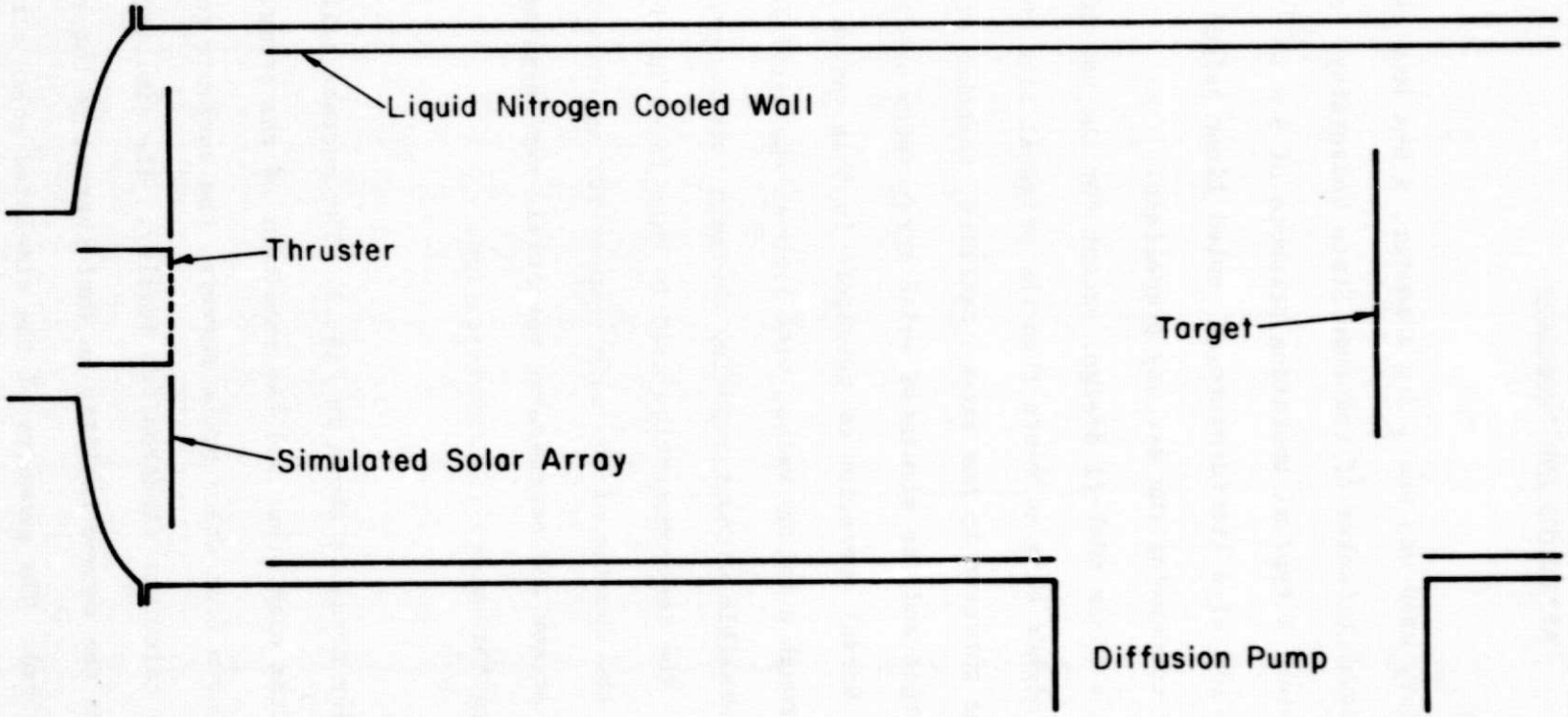

Fig. 1 - Sketch of Experimental Apparatus

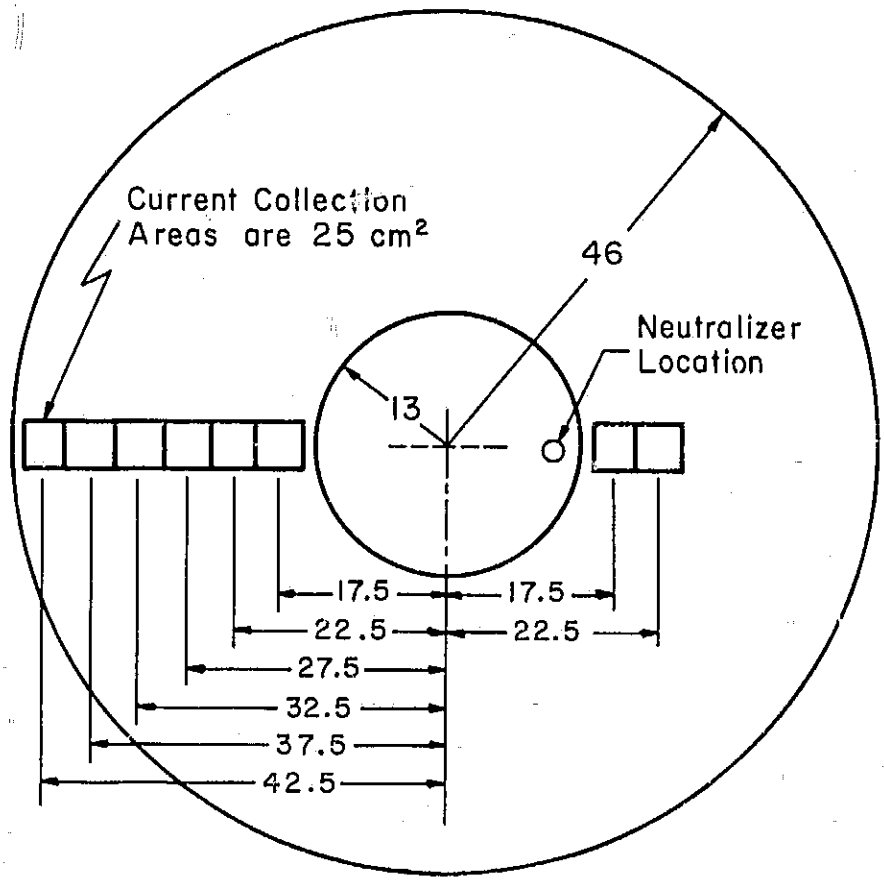

Fig. 2 - Sketch of Simulated Solar Array
All Dimensions in cm.

selected to facilitate analysis rather than as an approximation of any realistic spacecraft geometry.

The probe designs used in this investigation are shown in Fig. 3. Another design (similar to the one shown in Fig. 3(a), but only 1 cm long) was used in some initial tests, but no data obtained with this early design are included herein. The design of Fig. 3(a) was selected to offset the large Debye shielding distance found in the charge-exchange plasma surrounding the ion beam. Within the ion beam, the shielding distance is typically less than 1 mm, while the distance outside the beam was up to 1 cm. The thick-sheath procedure used to reduce the data is described by Isaacson,[8] and uses the theory and methods of Chen[9] for the accelerating field case. The sheath may be large compared to the probe diameter, but for the two-dimensional approach to be valid, the probe length should be large compared to the sheath thickness. With a sheath thickness up to several times the Debye shielding distance, a probe should be at least several centimeters long to give valid results in the charge-exchange plasma outside the ion beam. The 10-cm length of the first design [Fig. 3(a)] was selected for just this reason. The guarded configuration used in the second design [Fig. 3(b)] was an attempt to further assure the two-dimensional nature of the sheath. Only the current to the center section of the second design was used to determine plasma properties. The three-dimensional effects were assumed to be limited to the end sections, which were operated at the same potential as the center section.

The first probe design was used for surveys with the simulated solar array flush with the downstream end of the thruster. The second design was

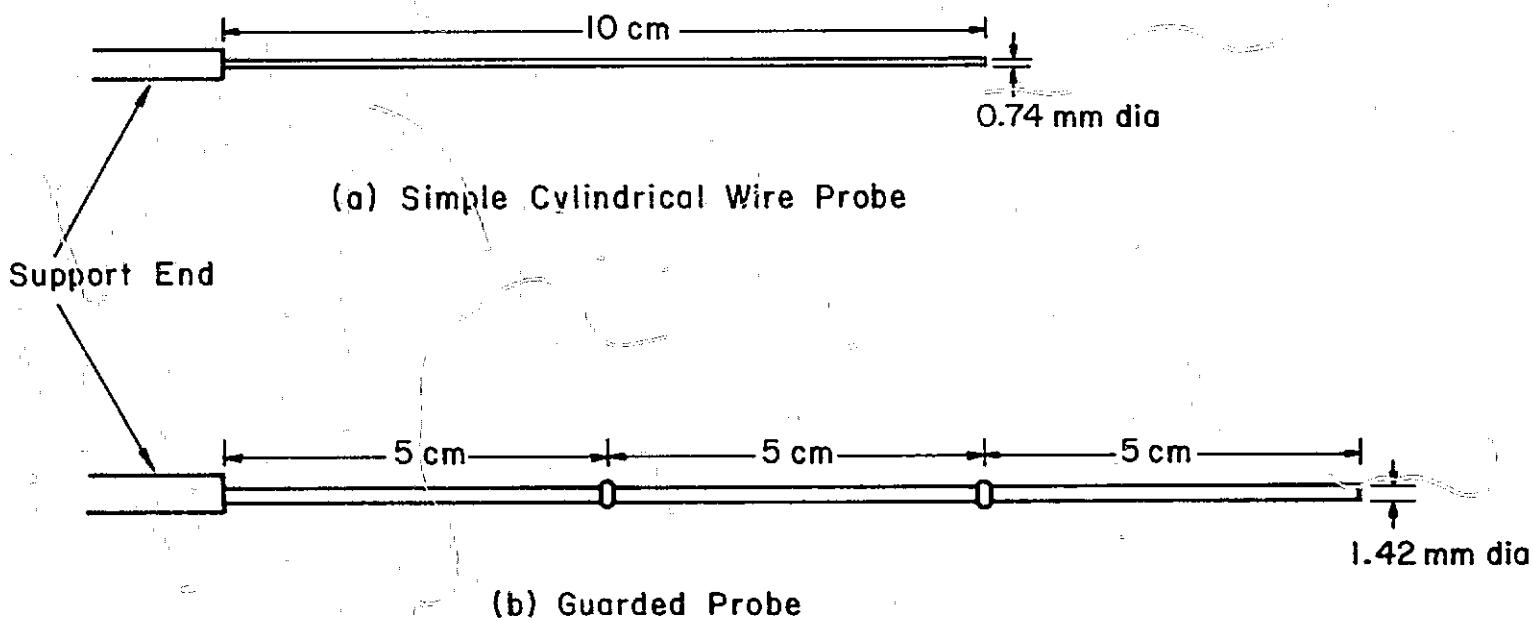

Fig. 3 - Plasma Probe Designs Used in Investigation

used for the surveys without the simulated array. While the first design could be operated throughout the survey region, the second design could only be operated in the charge-exchange plasma surrounding the ion beam. Attempted operation within the ion beam resulted in excessive total currents probably due to the larger probe surface area. Similar thruster operating conditions were used with and without the simulated array, so that beam surveys with the array could be substituted for the missing beam region with negligible error. These experiences with different probe designs indicate that it is difficult to obtain valid data in a wide range of plasma densities with one probe design.

Simulation of Space Environment

To most closely approximate the space environment, the vacuum facility was negative relative to the charge-exchange plasma. This potential difference avoided the reflection of ions at the facility boundaries. In space, of course, the charge-exchange ions would have continued indefinitely outwards from the region of the thruster. The electrons were reflected by the negative boundary, which was a closer approximation of space than the collection of all arriving electrons by a positive surface. In space there is an electron drift velocity (usually much smaller than electron random velocity) that gives zero net current from the spacecraft. The neutralizer was biased relative to the target to give an electron emission equal to the ion beam current. The exact distribution of electron drift velocity throughout the plasma volume was, of course, not the same as would have been obtained in space.

The negative facility bias was established by operating the target (see Fig. 1) at +60 volts relative to the facility. Because the dense plasma of the ion beam is an excellent conductor, the plasma potential is established by the target potential. All plasma potentials are measured relative to the target potential.

Another aspect of space simulation is the pressure level obtained in the facility. The liquid-nitrogen cooled wall should maintain the partial pressure of the mercury propellant at a sufficiently low value. To determine if the background pressure due to leakage was significant, air was bled into the facility at several different rates. The effect of changing facility pressure in this manner upon measured electron/ion density is indicated in Fig. 4. The variation of electron-ion density is small near the normal operating pressure of 5×10^{-6} torr, indicating that a further pressure reduction would not result in much change. Also, the data shown in Fig. 4 were obtained well downstream (32 cm downstream at a radius of 35 cm). Because the pressure of mercury due to the thruster decreases rapidly with distance from the thruster, such a downstream location is the most sensitive to background pressure. In support of this viewpoint, data obtained at an axial location closer to the thruster showed a much smaller effect of background pressure.

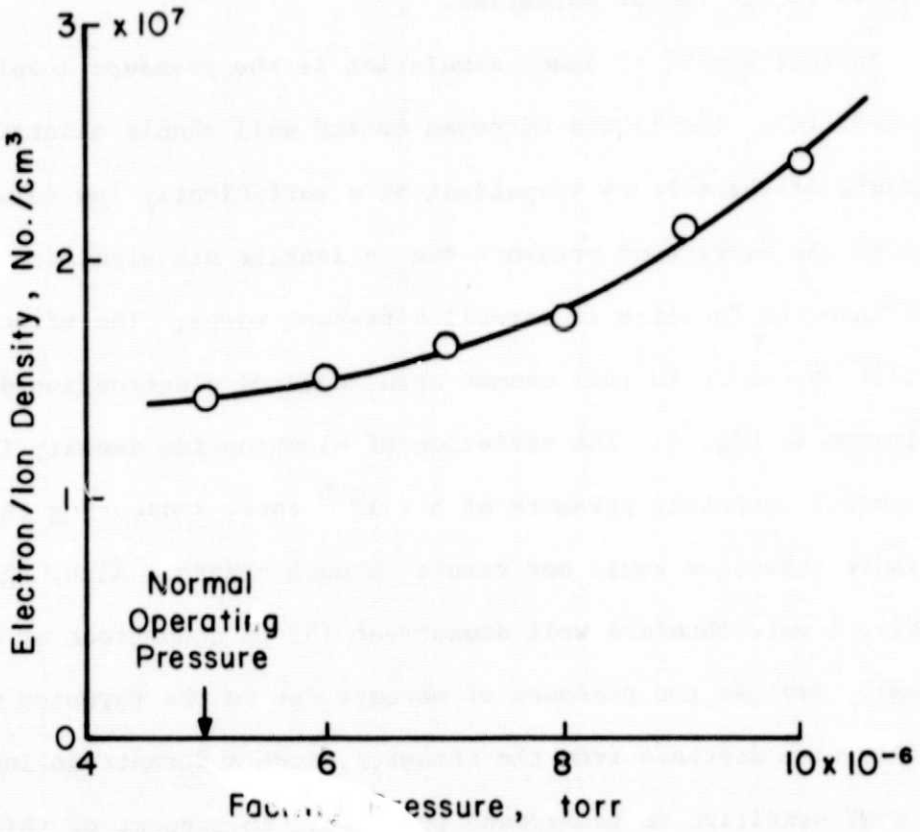

Fig. 4 - Effect of Air Bieed on Electron / Ion Density.

EXPERIMENTAL RESULTS

The basic problem of interaction between the ion thruster and a positive-potential solar array is indicated in Fig. 5. Small positive potentials were sufficient to draw a large electron current to any substantial surface area near a thruster. The magnitude of this electron current results from the high mobility of electrons. In comparison, the ion current produced by a negative potential is much smaller (also shown in Fig. 5). The source of the electron and ion currents shown in Fig. 5 is the charge-exchange plasma surrounding the ion beam. A transverse survey of electron density gave the results indicated in Fig. 6. Because the Debye shielding distances are small relative to the dimensions involved, the ion densities are essentially equal to the electron densities. Near the axis of the ion beam, the measured densities result primarily from energetic beam ions and their neutralizing electrons. In addition to ions, though, there are also neutrals leaving the thruster. When beam ions pass near slow moving neutral atoms, electrons can pass from the neutrals to the ions. This results in fast neutrals and slow ions. The fast neutrals rapidly leave the vicinity and are no problem. The slow ions produce a charge-exchange plasma that surrounds the ion beam. The charge-exchange ions constitute the majority beyond a radial distance of about 15 cm in the survey shown in Fig. 6. This charge-exchange plasma flows radially outwards from the beam at a low velocity relative to beam ions. Except for regions protected by a solid or fine-meshed screening electrode, the charge exchange plasma fills (with varying densities) all volume surrounding a thruster. A fine-meshed screen is defined as one in which the mesh dimension is equal to, or smaller than, the local Debye shielding distance.

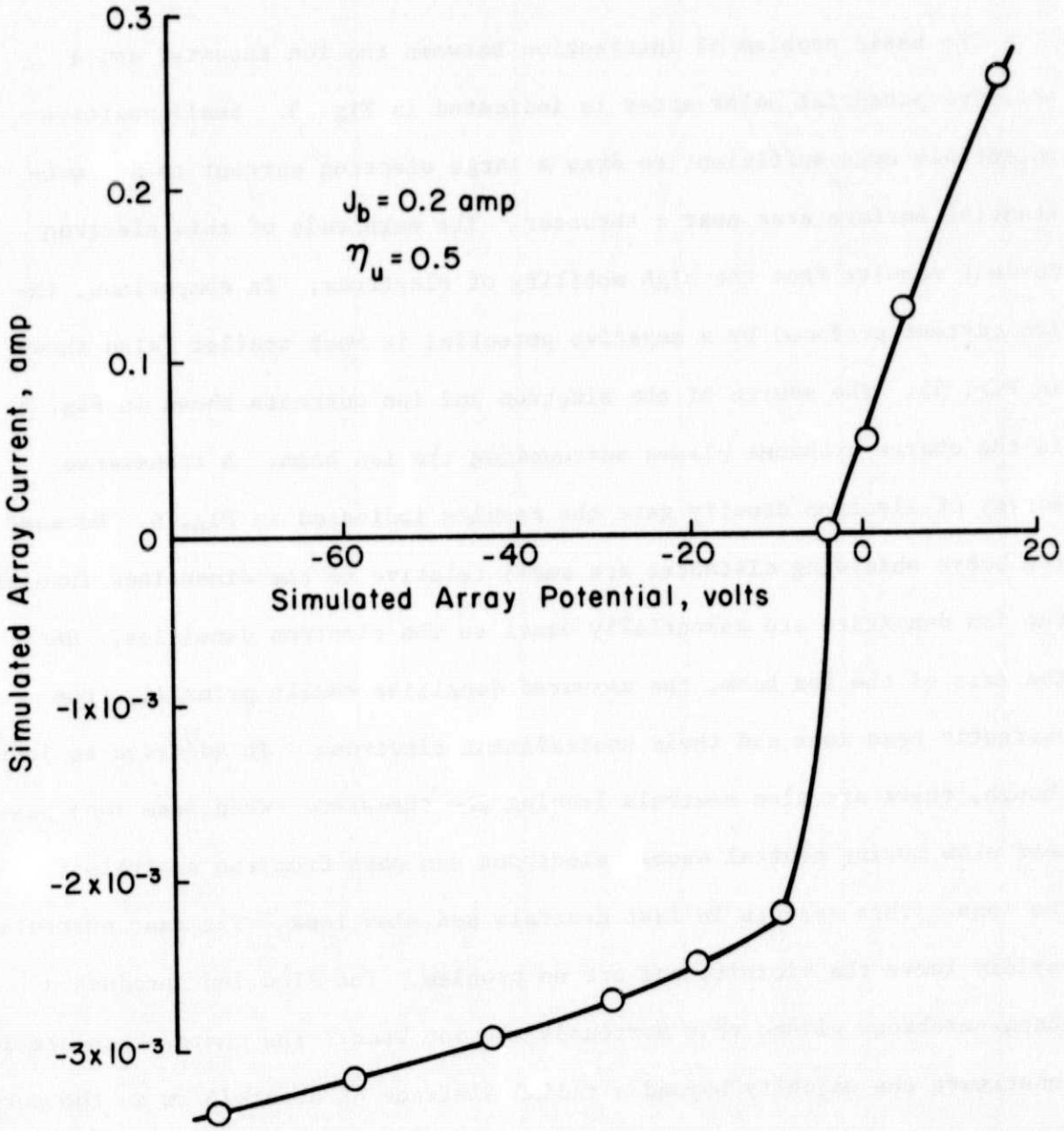

Fig. 5 - Effect of Potential on Current Collected by Simulated Solar Array.

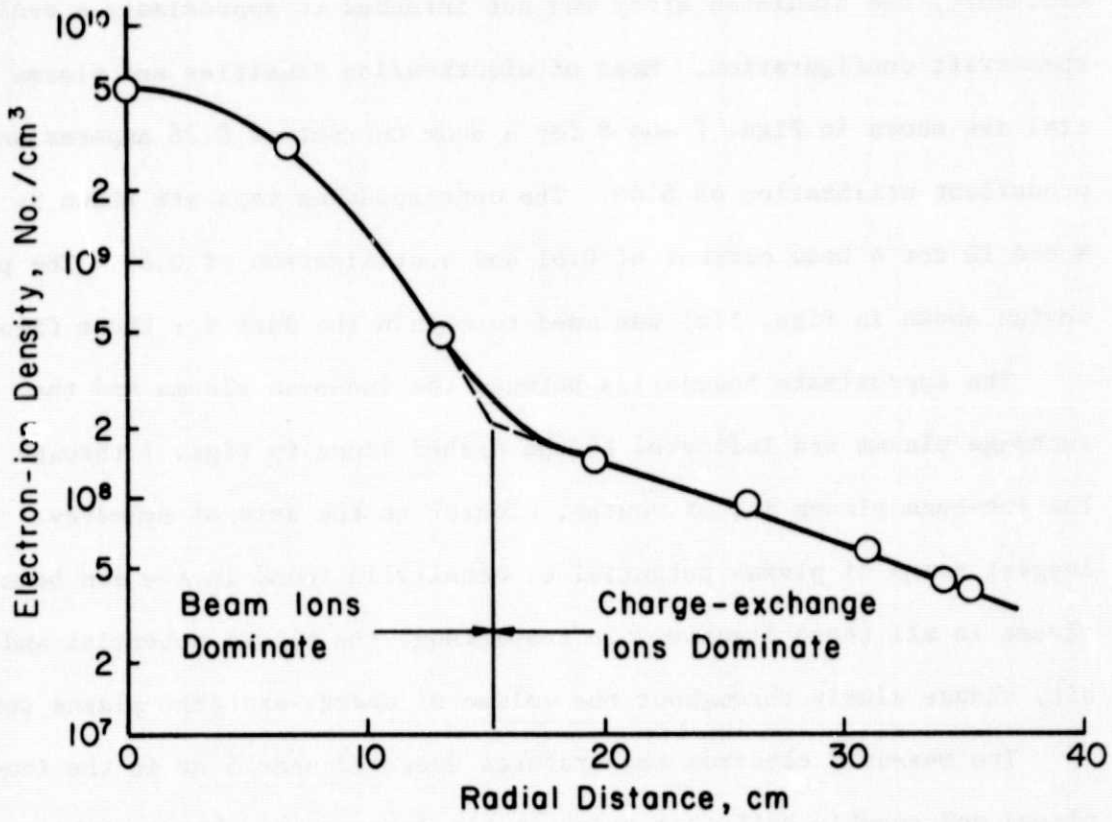

Fig. 6 - Separation of Plasma into Ion-beam and Charge-exchange Regions.

Surveys with Simulated Array

The first surveys were conducted with the simulated solar array flush with the downstream end of the thruster. As mentioned in Apparatus and Procedure, the simulated array was not intended to approximate a realistic spacecraft configuration. Maps of electron/ion densities and plasma potential are shown in Figs. 7 and 8 for a beam current of 0.36 amperes and a propellant utilization of 0.49. The corresponding maps are shown in Figs. 9 and 10 for a beam current of 0.61 and a utilization of 0.83. The probe design shown in Figs. 3(a) was used to obtain the data for these figures.

The approximate boundaries between the ion-beam plasma and the charge-exchange plasma are indicated by the dashed lines in Figs. 7 through 10. The ion-beam plasma is, of course, closest to the axis of symmetry. The largest range of plasma potential or density is found in the ion beam plasma in all these figures. In comparison, the plasma potential and density change slowly throughout the volume of charge-exchange plasma surveyed.

The measured electron temperatures averaged near 5 ev in the ion-beam plasma and roughly half that value in the surrounding charge-exchange plasma. The electron temperature, though, was felt to be the least reliable and reproducible of the plasma properties obtained from probe traces. (The densities were the most reproducible.) The plasma potential has been found by Sellen, et al.[1], to be related to plasma density through the barometric equation and the electron temperature, at least in the ion-beam plasma. The barometric equation can, therefore, be used to deduce electron temperature from potential-density plots, such as shown in Figs. 11 and 12. As should be expected, a clear trend of about 5 ev is indicated for the ion-beam

Surveys with Simulated Array

The first surveys were conducted with the simulated solar array flush with the downstream end of the thruster. As mentioned in Apparatus and Procedure, the simulated array was not intended to approximate a realistic spacecraft configuration. Maps of electron/ion densities and plasma potential are shown in Figs. 7 and 8 for a beam current of 0.36 amperes and a propellant utilization of 0.49. The corresponding maps are shown in Figs. 9 and 10 for a beam current of 0.61 and a utilization of 0.83. The probe design shown in Figs. 3(a) was used to obtain the data for these figures.

The approximate boundaries between the ion-beam plasma and the charge-exchange plasma are indicated by the dashed lines in Figs. 7 through 10. The ion-beam plasma is, of course, closest to the axis of symmetry. The largest range of plasma potential or density is found in the ion beam plasma in all these figures. In comparison, the plasma potential and density change slowly throughout the volume of charge-exchange plasma surveyed.

The measured electron temperatures averaged near 5 ev in the ion-beam plasma and roughly half that value in the surrounding charge-exchange plasma. The electron temperature, though, was felt to be the least reliable and reproducible of the plasma properties obtained from probe traces. (The densities were the most reproducible.) The plasma potential has been found by Sellen, et al.[1], to be related to plasma density through the barometric equation and the electron temperature, at least in the ion-beam plasma. The barometric equation can, therefore, be used to deduce electron temperature from potential-density plots, such as shown in Figs. 11 and 12. As should be expected, a clear trend of about 5 ev is indicated for the ion-beam

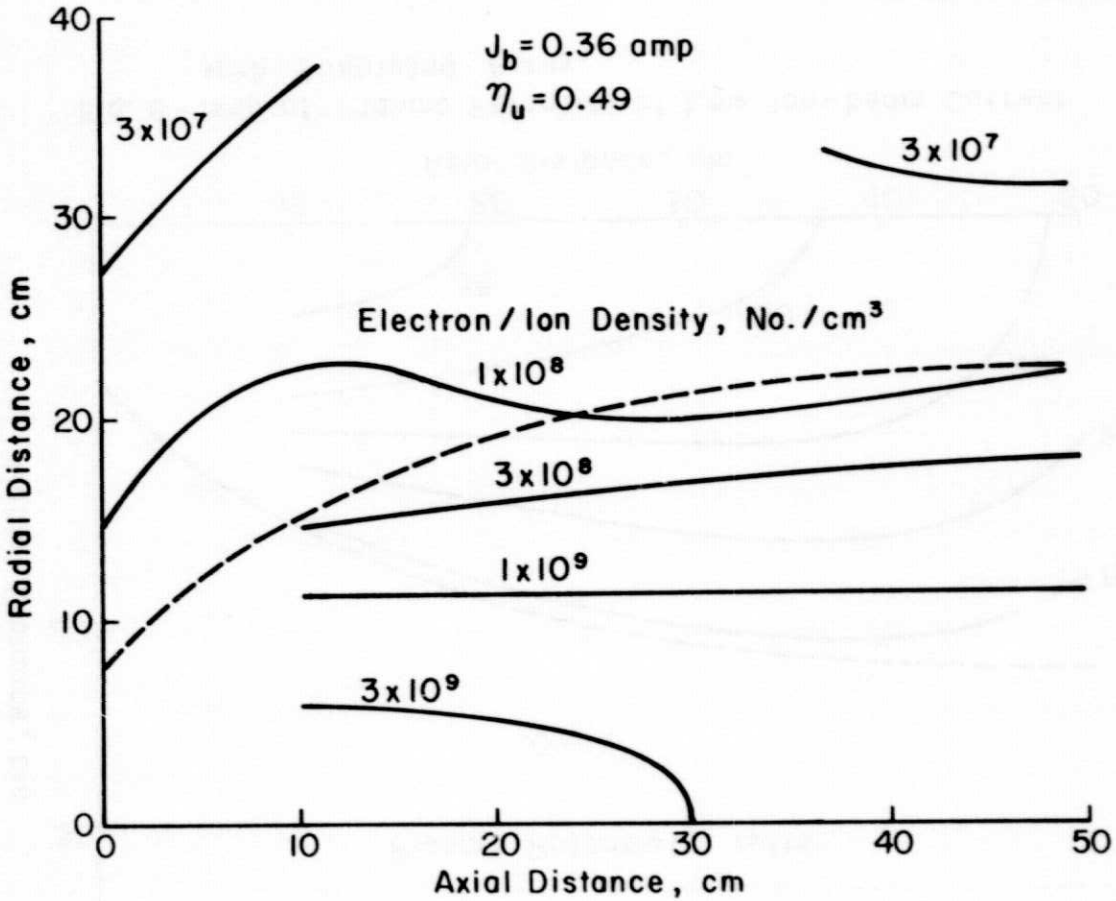

Fig. 7 - Map of Electron / Ion Density at Low Ion-beam Current with Simulated Array.

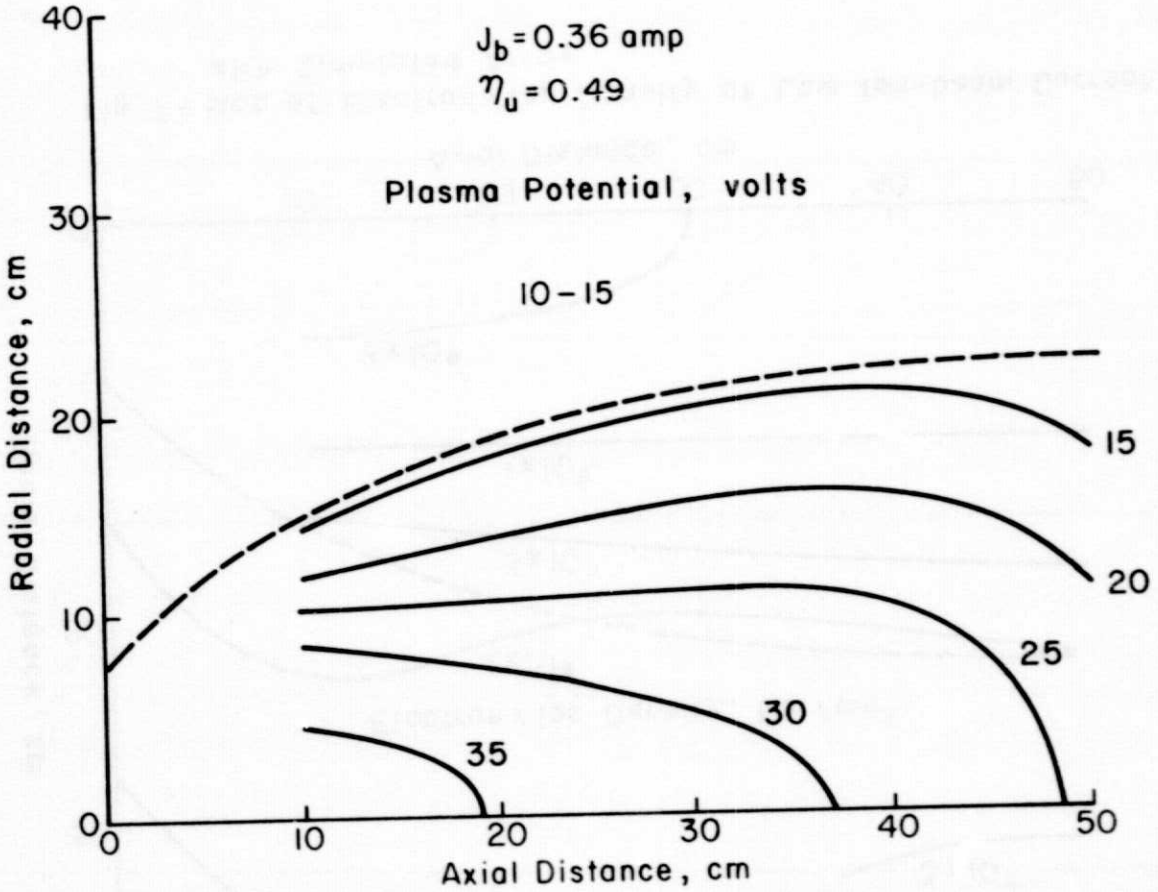

Fig. 8 - Map of Plasma Potential at Low Ion-beam Current with Simulated Array.

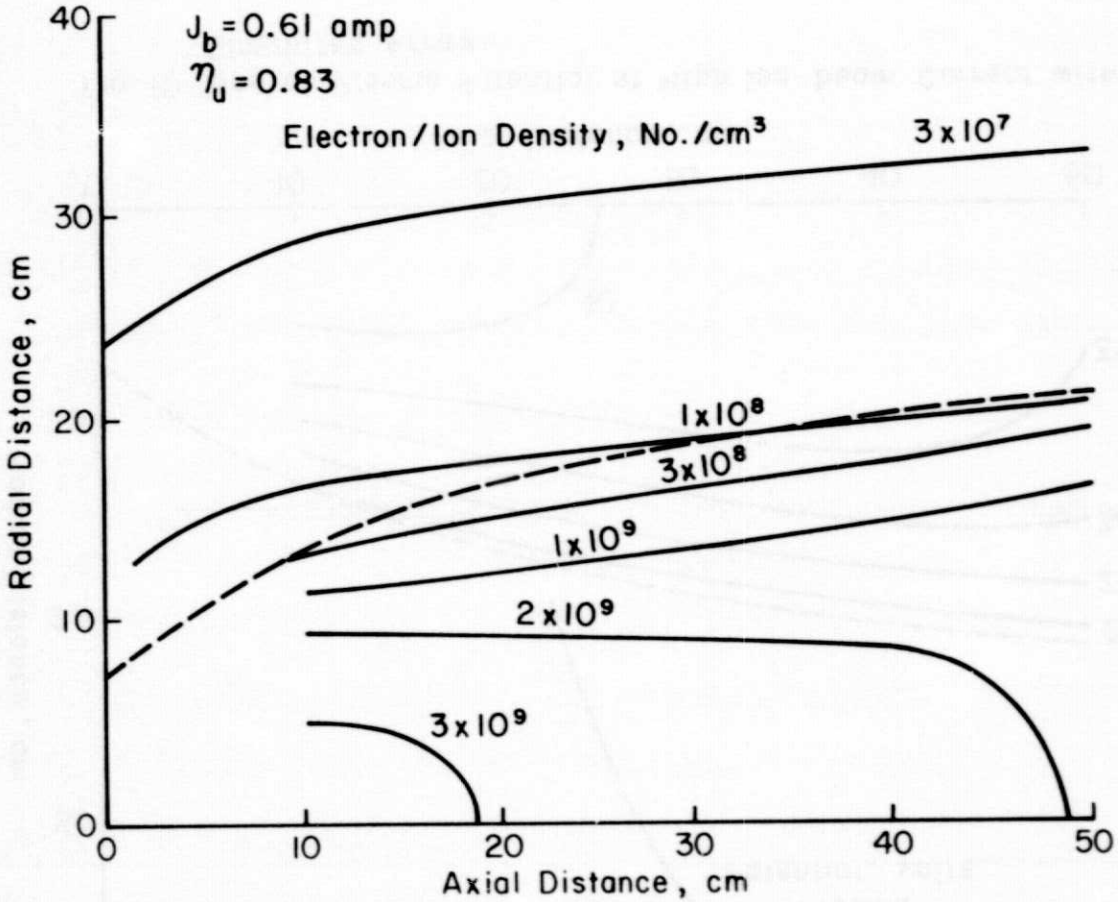

Fig. 9 - Map of Electron / Ion Density at High Ion-beam Current with Simulated Array.

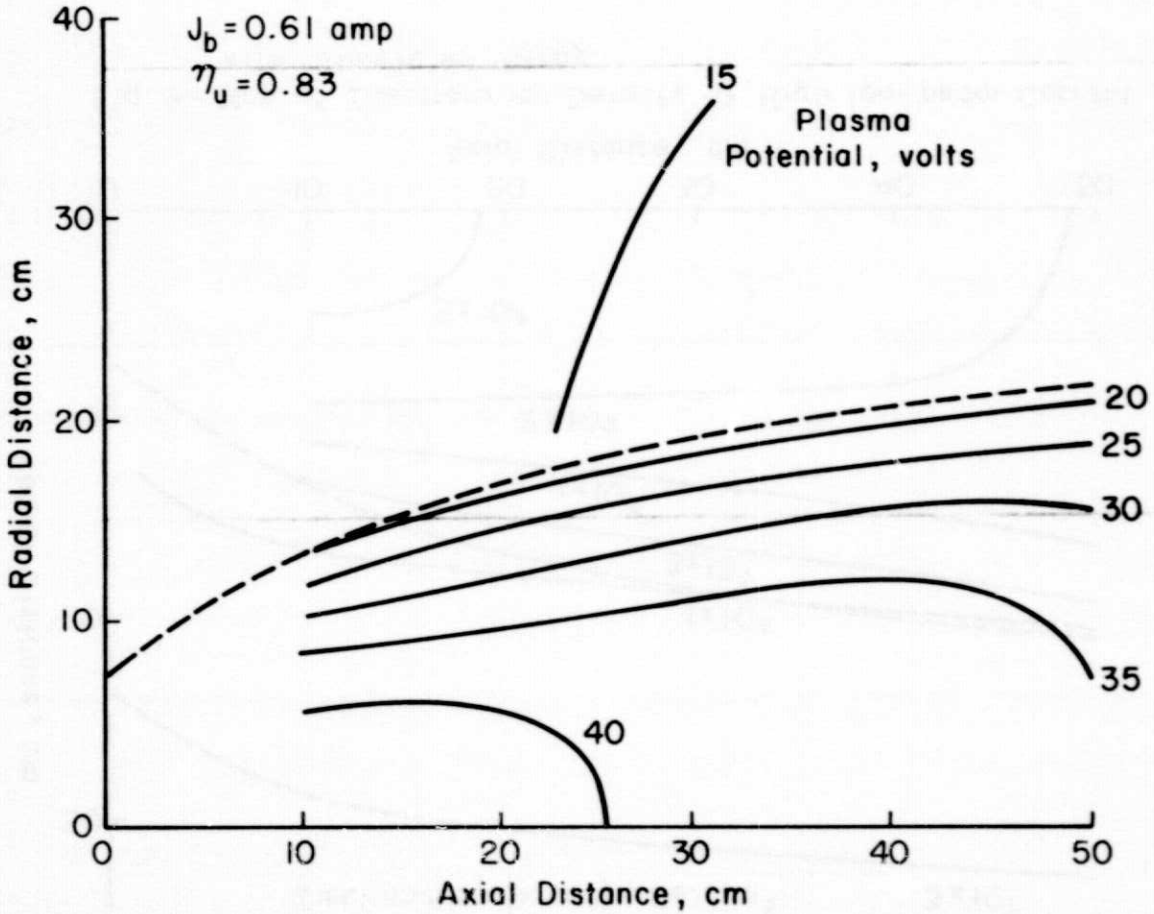

Fig. 10-Map of Plasma Potential at High Ion-beam Current with Simulated Array.

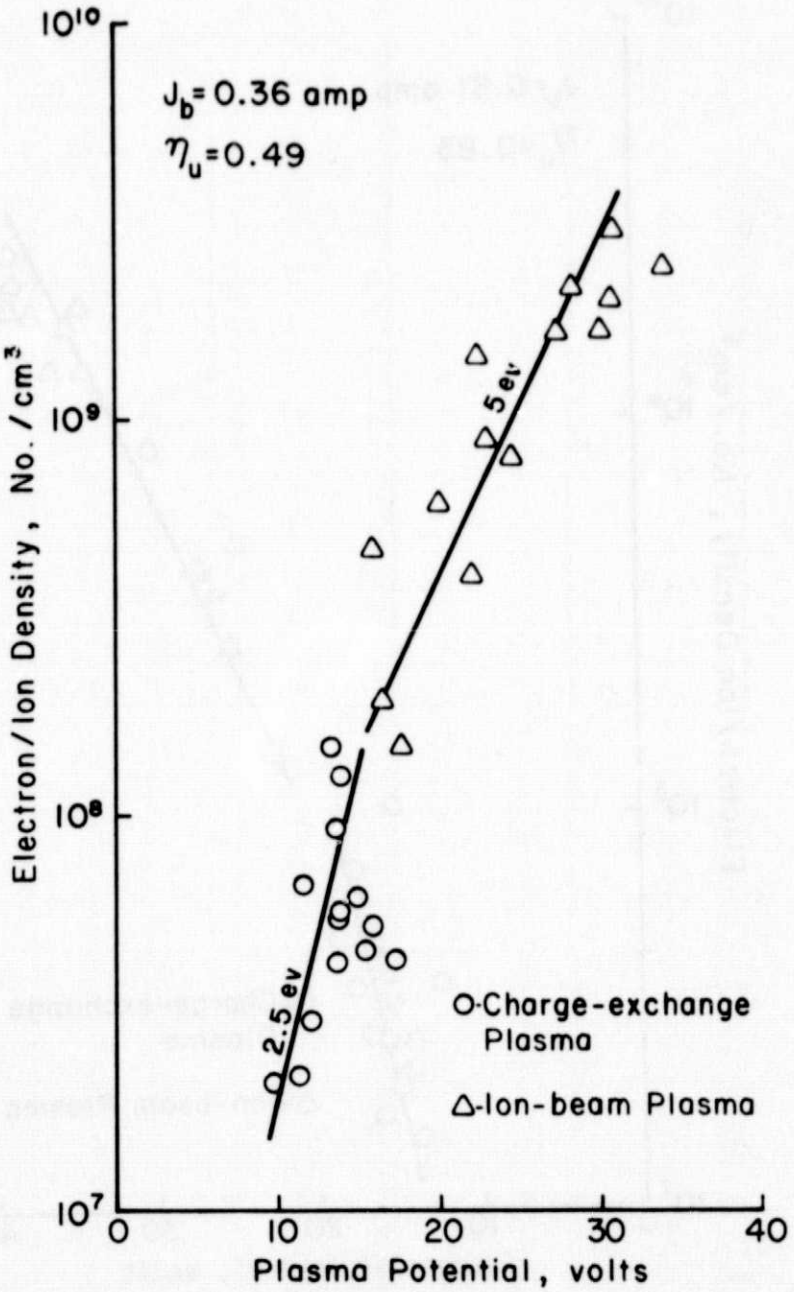

Fig. 11 - Check on Barometric Equation at Low Ion-beam Current with Simulated Array.

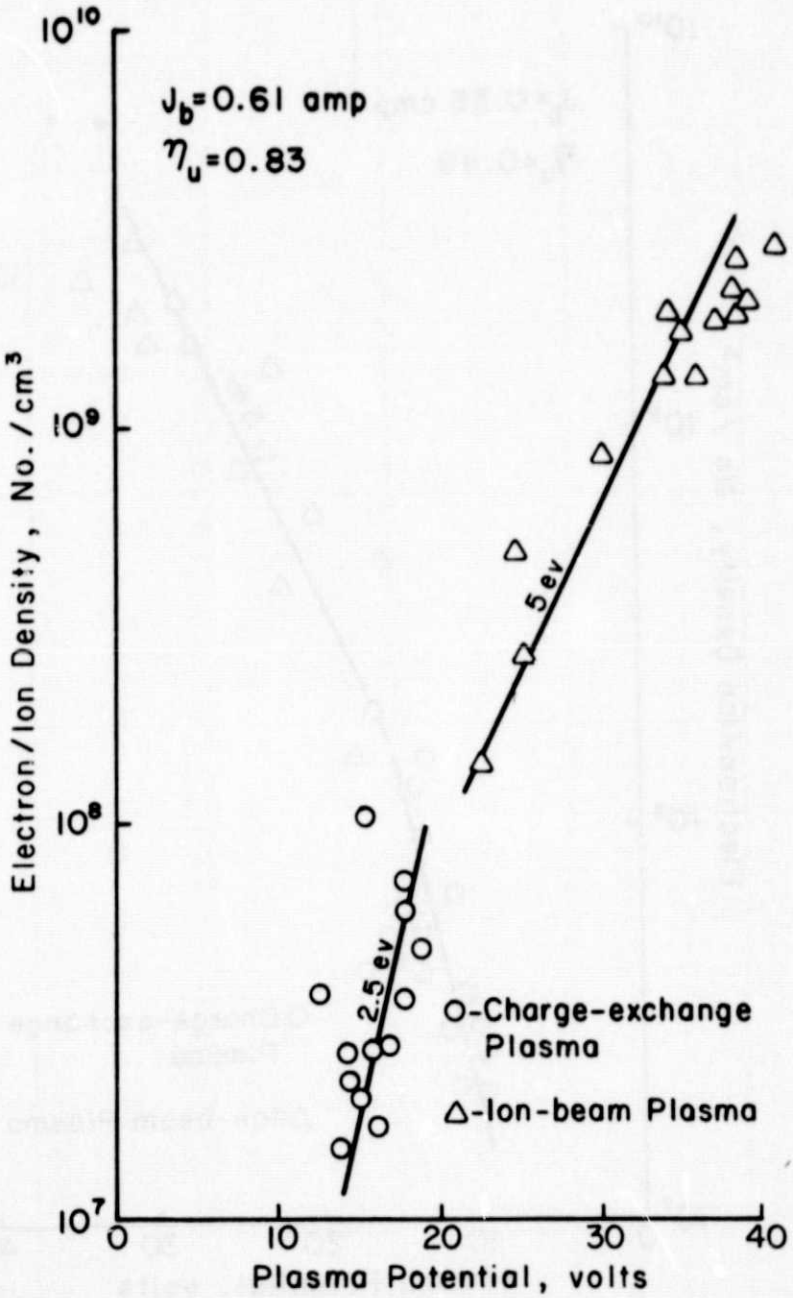

Fig. 12 – Check on Barometric Equation at High Ion-beam Current with Simulated Array.

plasma in these figures. There is also some indication that the barometric equation describes the potential density variation in the charge-exchange plasma with a temperature of roughly 2.5 ev. The small range of density covered, together with the uncertainty in plasma potential, though, makes the validity of the barometric equation more questionable in the charge-exchange plasma. Tests without the simulated solar array fortunately resulted in a wider range of density for the charge-exchange plasma, so the validity of the barometric equation will be re-examined in the next section.

Surveys without Simulated Array

Surveys were also made with the simulated solar array removed. This was done to evaluate the extent to which charge-exchange ions are deflected upstream of the thruster. To improve the two-dimensional probe-sheath approximation, the probe design shown in Fig. 3(b) was used for these surveys. Although this design was (and is) felt to give more accurate results in a low density charge-exchange plasma, it also resulted in excessive total probe currents in the ion-beam plasma. Probe data, therefore, could not be obtained within the ion beam. Operating conditions were close to those used for Figs. 7 through 10, so data obtained from these earlier tests were used for the ion-beam plasma in the next four figures.

Maps of electron/ion densities and plasma potential are shown in Figs. 13 and 14 for an ion beam current of 0.38 amperes and a propellant utilization of 0.51. The corresponding maps for 0.63 amps and 0.85 utilization are shown in Figs. 15 and 16.

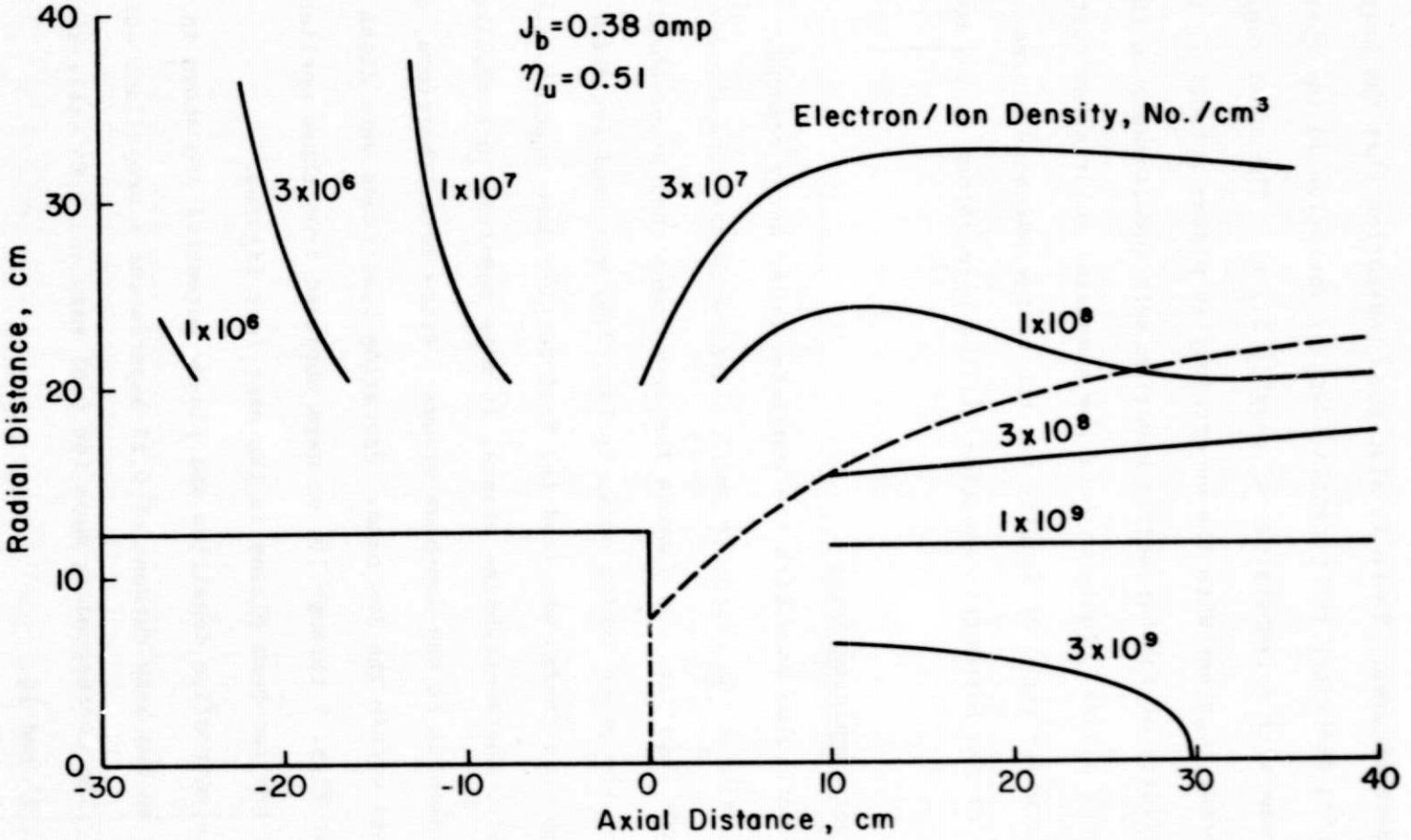

Fig. 13 - Map of Electron/Ion Density at Low Ion-beam Current without Simulated Array.

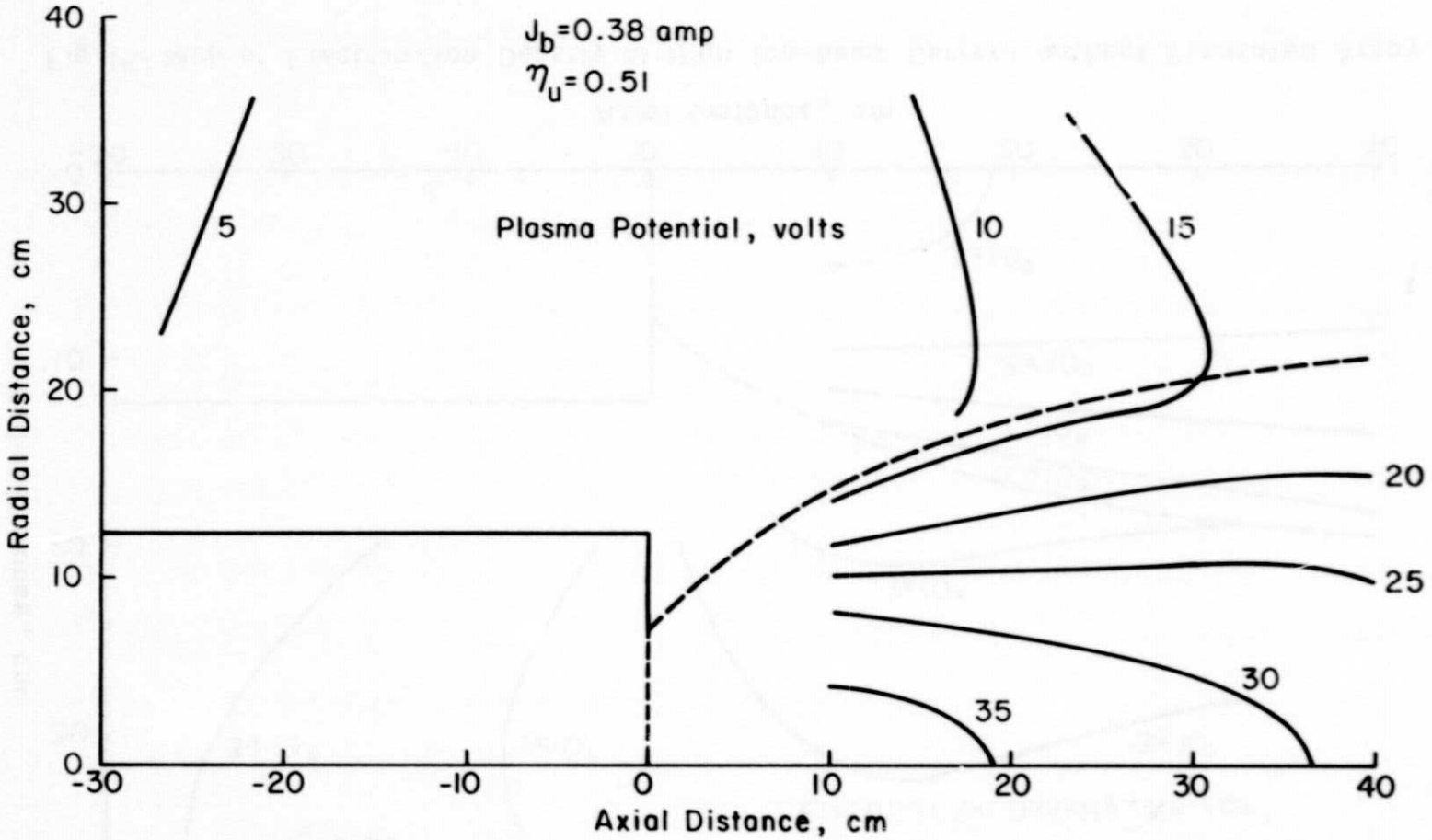

Fig. 14 - Map of Plasma Potential at Low Ion-beam Current without Simulated Array.

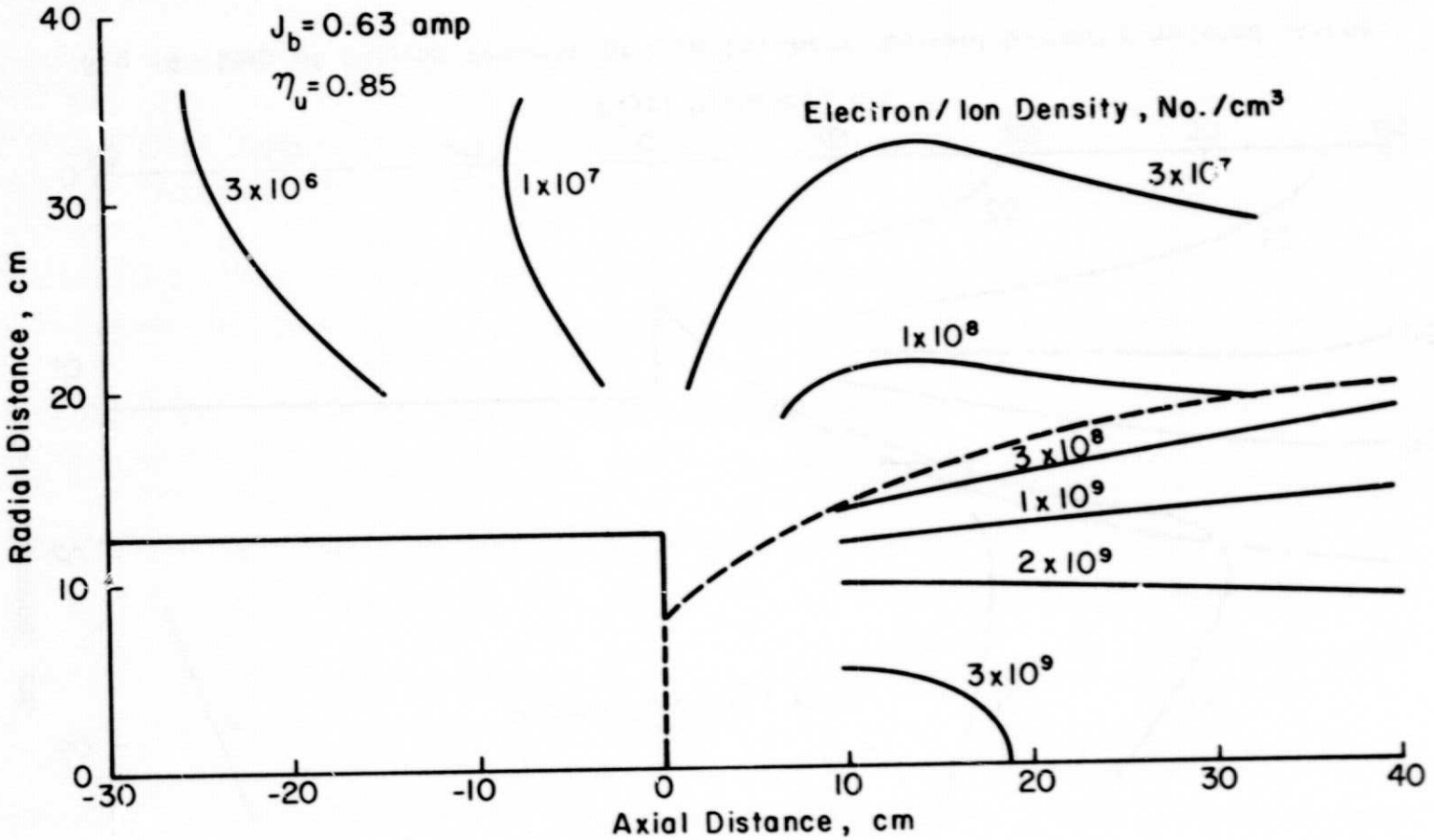

Fig. 15- Map of Electron/Ion Density at High Ion-beam Current without Simulated Array

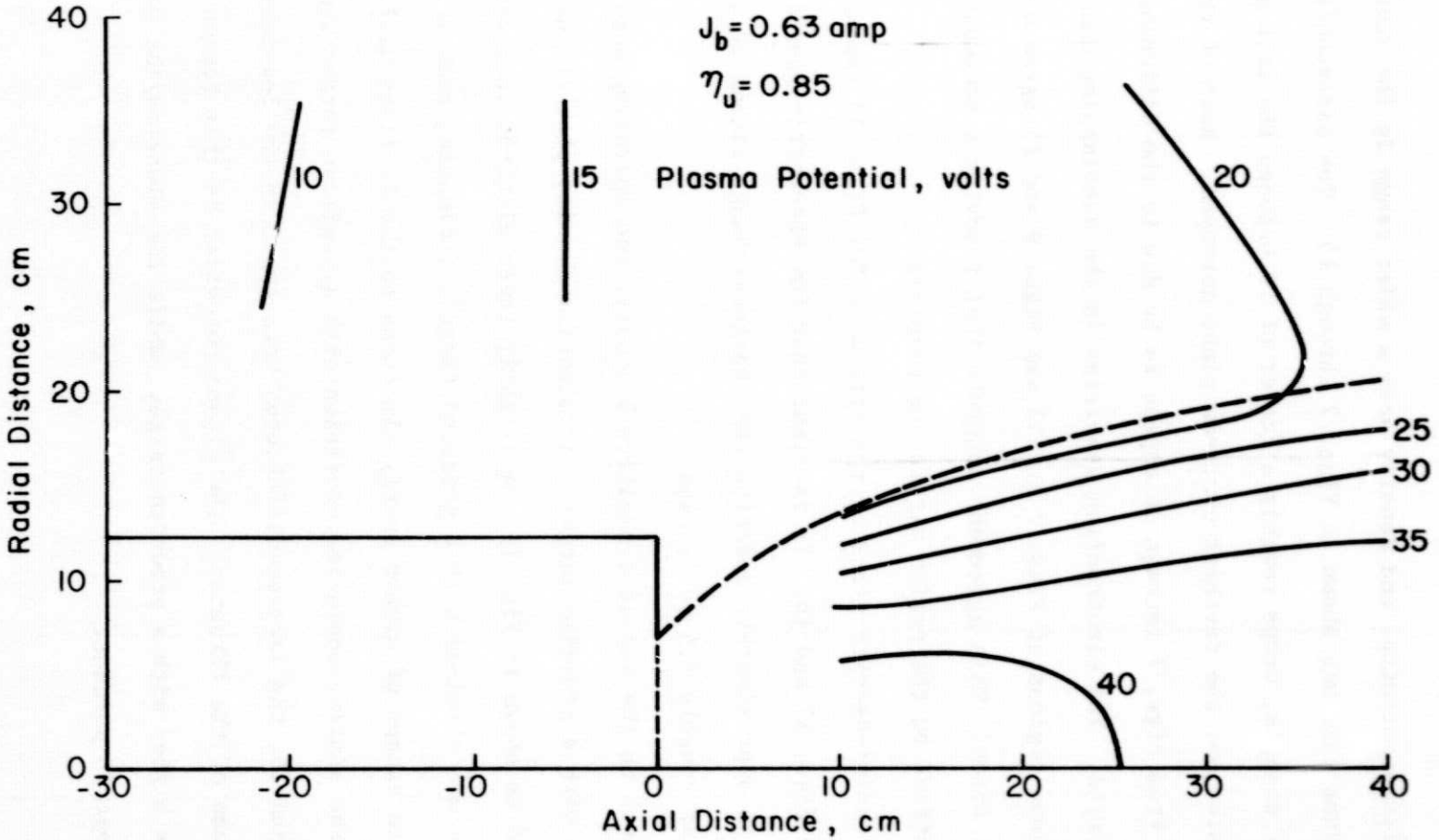

Fig. 16 - Map of Plasma Potential at High Ion-beam Current without Simulated Array.

Both plasma potential and density show a wider range in the charge-exchange plasma than was shown in Figs. 7 through 10. The electron/ion density, for example, drops roughly a factor of 10 between the exit plane of the thruster and the farthest upstream plane surveyed. Most of the differences from Figs. 7 through 10 appear to be due to the different regions surveyed. The electron/ion densities in the overlapping charge-exchange plasma regions of Figs. 7 and 13 and Figs. 9 and 15 agree within experimental error. This agreement suggests that removing a boundary has little effect on the region within the boundary.

The potential-density plots of the data used for Figs. 13 through 16 are shown in Figs. 17 and 18. It is clear that the barometric equation can be used to approximately describe the charge-exchange plasma if a temperature of roughly 2.5 ev is used.

As a check on the use of a negative boundary, one operating condition was surveyed with a grounded target. A potential-density plot of the data obtained is shown in Fig. 19. A slightly lower electron temperature of about 2 ev was obtained with a grounded target, indicating some electron cooling due to escape of higher energy electrons to the facility wall. Compared to the similar operating condition with a positive target shown in Figs. 15 and 16, the largest differences were found in the low-density plasma upstream of the thruster. The plasma potential in this region was about 5 volts higher with a grounded target, while the electron/ion density increased about 60 percent.

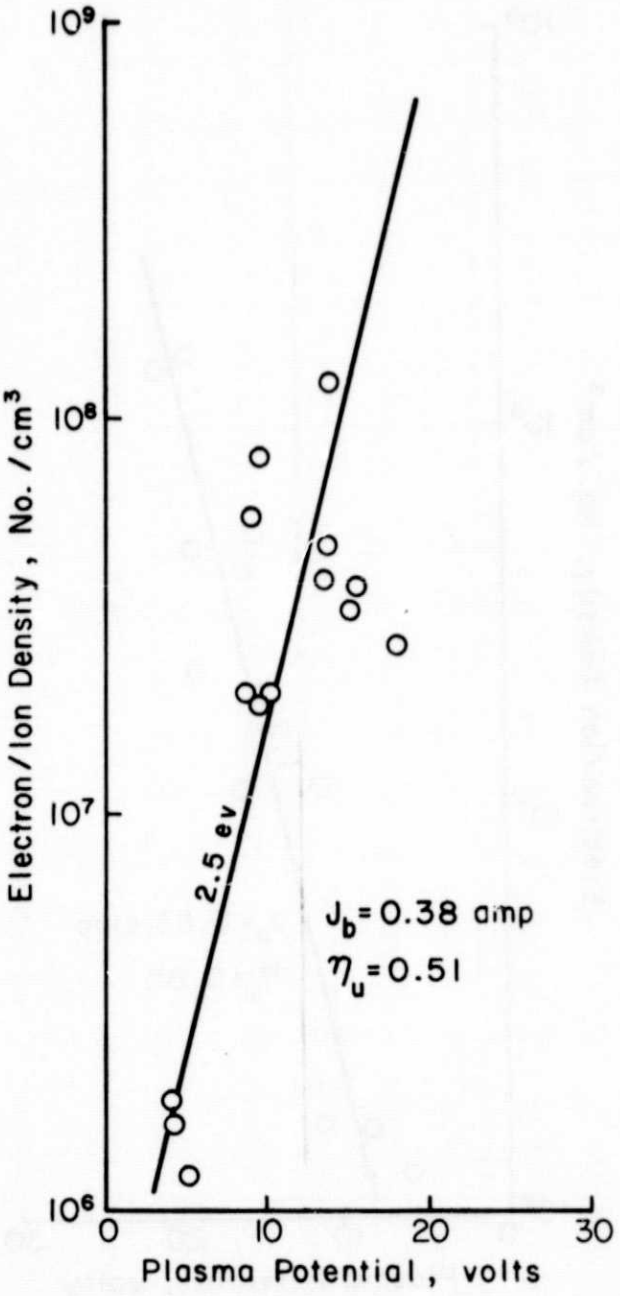

Fig. 17 - Check on Barometric Equation at Low Ion-beam Current without Simulated Array. (Charge-exchange Plasma Only.)

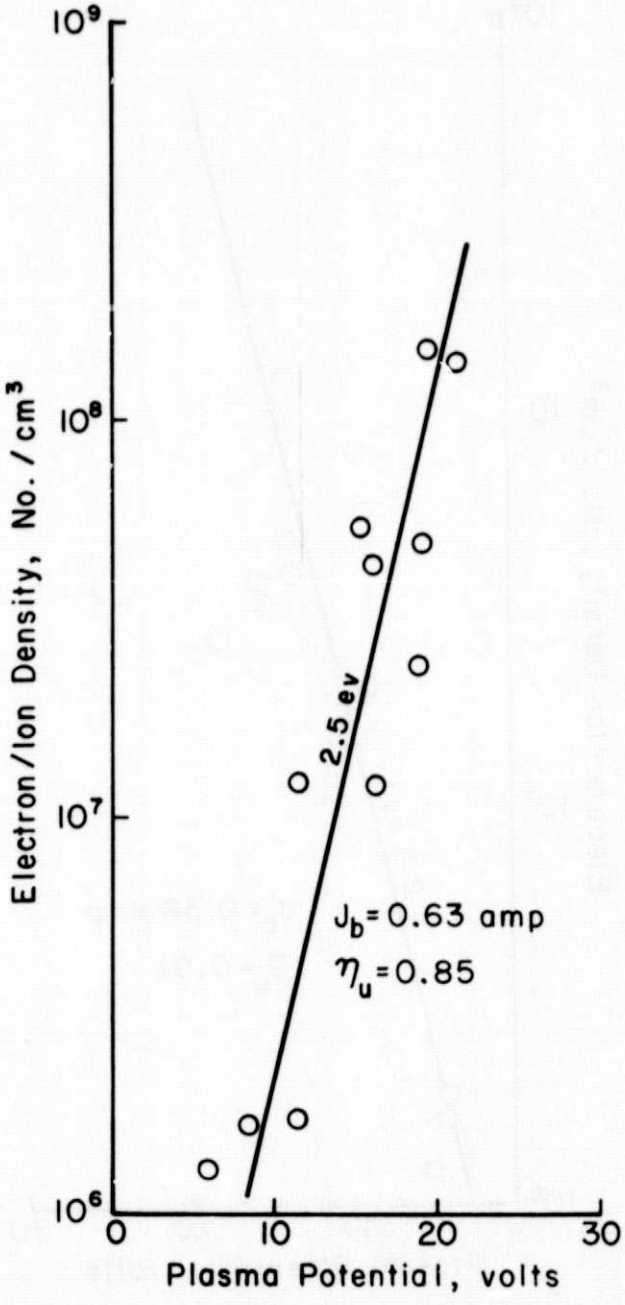

Fig. 18 - Check on Barometric Equation at High Ion-beam Current without Simulated Array. (Charge-exchange Plasma Only.)

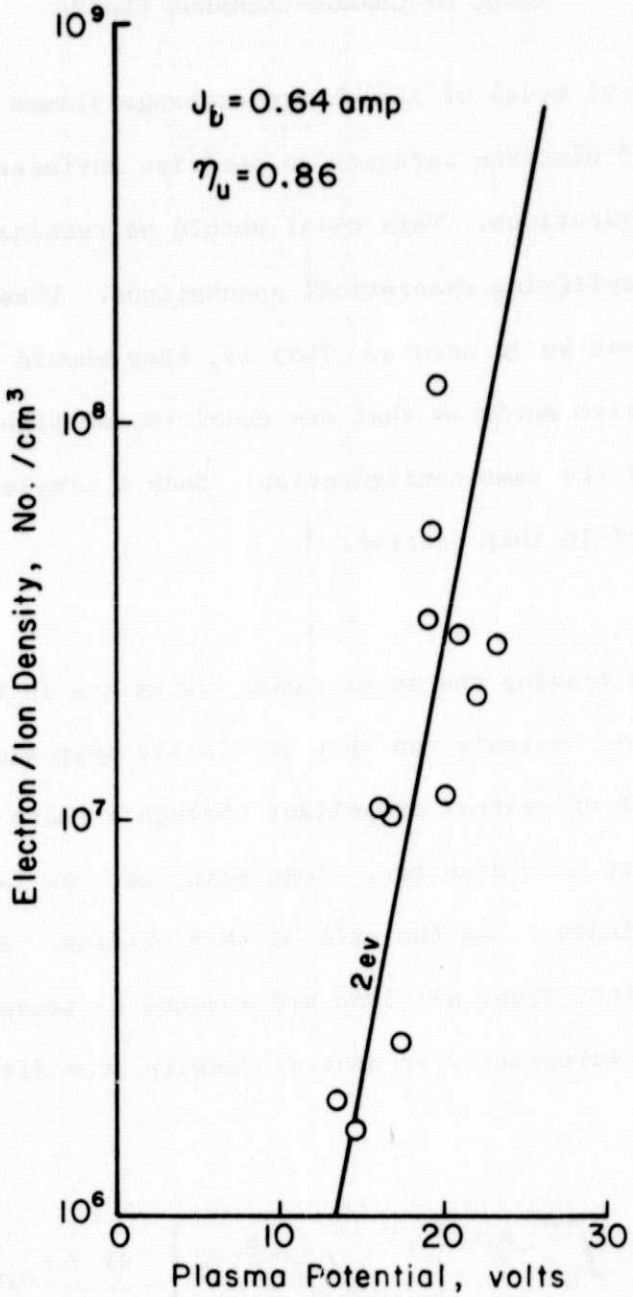

Fig. 19 - Check on Barometric Equation with Grounded Target. (Without Simulated Array.)

MODEL OF CHARGE-EXCHANGE PLASMA

A mathematical model of the charge-exchange plasma is desirable to make estimates of electron currents to positive surfaces for various spacecraft configurations. This model should be reasonably simple to use, which implies simplifying theoretical assumptions. These assumptions should be conservative in nature. That is, they should result in electron currents to positive surfaces that are equal to, or higher than, experimental values for the same configuration. Such a simple, conservative model is presented in this section.

Isotropic Model

The neutrals leaving the accelerator system are in free molecular flow. The distribution of neutrals can thus be closely approximated by the flow of the same amount of neutral propellant through a sharp edged orifice with a diameter equal to beam diameter. Ions pass near the largest number of neutrals if they leave along the axis of this orifice. In the first conservative assumption, then, all ions are assumed to leave on the orifice (beam) axis. The integration of neutral density over distance along this axis yields

$$\int_o^\infty n_o dx = \int_o^\infty \frac{n_{o,r}}{2}\left[1 - \frac{x}{\sqrt{x^2 + r_b^2}}\right] dx = n_{o,r}\, r_b/2 , \qquad (2)$$

where x is the distance downstream of the orifice, r_b is the radius of the orifice (or beam), and $n_{o,r}$ is the reservoir density upstream of the orifice. This density $n_{o,r}$ is a calculated value that gives the correct loss rate of neutrals, $\dot{N}_o$,

$$\dot{N}_o = \pi r_b^2 \, n_{o,r} \, \bar{v}_o / 4 \, , \tag{3}$$

where $\bar{v}_o$ is the average neutral velocity, $\sqrt{8kT_o/\pi m_o}$. The charge-exchange production rate is thus

$$\dot{N}_{ce} = n_{o,r} \, r_b \, \sigma_{ce} \, \dot{N}_i / 2 \, , \tag{4}$$

with σ_{ce} the charge-exchange cross section. Expressed in terms of ion-beam current, J_b, and propellant utilization, η_u, the last equation becomes

$$\dot{N}_{ce} = \frac{2 \, J_b^2 (1 - \eta_u) \sigma_{ce}}{\pi \, r_b \, \eta_u \, q^2 \, \bar{v}_o} \, , \tag{5}$$

with q the magnitude of electronic charge. In the isotropic model these ions are assumed to be distributed equally in all radial directions from the effective source downstream of the thruster. This effective source is assumed to be one beam radius downstream of the accelerator system, although the exact location of this source will not be important at the usual radial distance for a solar array. The radial velocity is assumed to be the minimum that could be expected, to maximize ion density and, therefore, electron and electron current densities. This minimum velocity is the minimum ion velocity for a stable plasma sheath,

$$v_{ce} = \sqrt{kT_e/m_o} \, , \tag{6}$$

which was first obtained by Bohm.[10] The mass of the ion is essentially the mass of a propellant neutral, m_o, while k is the Boltzmann constant

and T_e is the electron temperature in the ion beam. The density of charge-exchange ions n_{ce} at radius R from the effective source is, therefore,

$$n_{ce} = \dot{N}_{ce}/4\pi R^2 v_{ce} \ . \tag{7}$$

The density of charge-exchange ions equals the density of electrons. Any positive surface will collect all the electrons that arrive at that surface. This electron current density is

$$j_e = n_{ce}\, \bar{v}_e\, q/4 \ , \tag{8}$$

where $\bar{v}_e$ is the average electron velocity in the charge-exchange plasma, $\sqrt{8kT_e'/\pi m_e}$. Note that T_e' is the electron temperature in the charge-exchange plasma, while T_e is in the ion beam. If we use the experimental observation that $T_e' \approx T_e/2$, then $\bar{v}_e$ can be expressed, $2\sqrt{kT_e/\pi m_e}$.

With all the numerical values of constants substituted, we can express the production rate, density and current density as

$$\dot{N}_{ce} = \frac{1.70 \times 10^{35}\, J_b^{\,2}(1 - \eta_u)\sigma_{ce}\sqrt{A}}{r_b\, \eta_u \sqrt{T_o}} \tag{9}$$

$$n_{ce} = \frac{1.49 \times 10^{32}\, J_b^{\,2}(1 - \eta_u)\sigma_{ce}\, A}{r_b\, R^2\, \eta_u \sqrt{T_o T_e}} \tag{10}$$

$$j_e = \frac{2.62 \times 10^{16}\, J_b^{\,2}(1 - \eta_u)\sigma_{ce}\, A}{r_b\, R^2\, \eta_u \sqrt{T_o}} \tag{11}$$

where T_o and T_e are in °K and A is the atomic weight of the propellant atoms. With the further typical value of 500°K used for T_o, these equations become

$$\dot{N}_{ce} = 7.62 \times 10^{33} J_b^2 (1 - \eta_u) \sigma_{ce} \sqrt{A}/r_b \eta_u , \quad (12)$$

$$n_{ce} = 6.65 \times 10^{30} J_b^2 (1 - \eta_u) \sigma_{ce} A/r_b R^2 \eta_u \sqrt{T_e} , \quad (13)$$

$$j_e = 1.17 \times 10^{15} J_b^2 (1 - \eta_u) \sigma_{ce} A/r_b R^2 \eta_u . \quad (14)$$

Typical propellants are mercury, cesium, xenon, and argon, for which the charge-exchange cross sections at 1000 ev are about 6×10^{-19},[11-13] 2×10^{-18},[14] 4.5×10^{-19},[11,12,15] and $2.5 \times 10^{-19} m^2$.[11,12,15] These values change slowly with ion energy, with the mercury value increasing to only about $8 \times 10^{-19} m^2$ at 100 ev. Substituting the value of 5 ev (58,000 °K) for the T_e observed with mercury, as well as an atomic weight of 200.6, the equations become

$$\dot{N}_{ce} = 6.5 \times 10^{16} J_b^2 (1 - \eta_u)/r_b \eta_u , \quad (15)$$

$$n_{ce} = 3.3 \times 10^{12} J_b^2 (1 - \eta_u)/r_b R^2 \eta_u , \quad (16)$$

$$j_e = .14 J_b^2 (1 - \eta_u)/r_b R^2 \eta_u . \quad (17)$$

It should be noted that lower values of T_e were obtained by Komatsu, et al.[5], but the value obtained here is consistent with the usual mercury hollow-cathode injection voltage of about 20 and the ratio of 0.3 for

electron temperature divided by this voltage, which was found by Ogawa, et al.[2,3] Xenon and argon would be expected to have roughly the same electron temperature as mercury, while the lower excitation energy of cesium should result in a lower value. Worlock, et al. found a T_e of 0.4 ev for a cesium bombardment thruster with a hollow-cathode neutralizer.[7]

Angular Dependence Model

Measuring the angle from the beam direction, the range from 0 to 90° is assumed to be given by the isotropic model. The range from 90 to 180° involves bending trajectories behind the plane of the thruster and is of interest in this section. Examination of Figs. 14 and 16 shows that, close to the thruster, ions leave at approximately 90°. In the charge-exchange plasma region, equipotentials near, and upstream of, the accelerator system are approximately normal to the beam direction. Thus the electric field in this region is approximately antiparallel to beam direction.

A simple model for bending charge-exchange ion trajectories in the 90 to 180° range can be derived by assuming that ions initially moving in the 90° direction are deflected by an electric field opposite to beam direction. The same minimum ion velocity, $\sqrt{kT_e/m_o}$, is used as the initial velocity in the 90° direction. This velocity is equivalent to an accelerating potential difference of $kT_e/2q$. For the upstream direction, a potential difference of ΔV is used. The 90 and 180° velocity components are related to these two potential differences,

$$2q\Delta V/kT_e = v_{180}^2/v_{90}^2 = \text{ctn}^2\theta \ , \qquad (18)$$

with θ restricted to the 90 to 180° range. The barometric relationship in the charge-exchange plasma is

$$n_{ce}/n_{ce,90} = \text{Exp}[-q\Delta V/kT_e'] \quad . \tag{19}$$

Again using half T_e as T_e', we have

$$n_{ce}/n_{ce,90} = \text{Exp}[-2q\Delta V/kT_e] \quad . \tag{20}$$

Substitution of Eq. (18) into Eq. (20) yields

$$n_{ce}/n_{ce,90} = \text{Exp}[-ctn^2\theta] \quad , \tag{21}$$

with θ again restricted to the 90 to 180° range. Eq. (21), then, is the desired variation with angle. Inasmuch as electron current density also depends linearly on electron/ion density, the current density equations must also be multiplied by the ratio of $n_{ce}/n_{ce,90}$.

Comparison with Experiment

Theoretical and experimental electron/ion densities are compared in Figs. 20 and 21. In Figs. 20 the comparison is in the plane normal to the ion beam (constant 90° direction). In Figs. 21 the comparison is at a constant radial distance (34 cm) and a variable direction. In both cases the angle and radial distance are measured from a point one beam radius downstream of the center of the accelerator system.

The agreement of theoretical and experimental densities is reasonable (and conservative) over most of the ranges covered by Figs. 20 and 21. The exception is at angles less than 90° from the beam direction. Examination of experimental equipotential contours within the ion beam (Figs. 8 and 10) will show that charge-exchange ions receive initial velocities in mostly

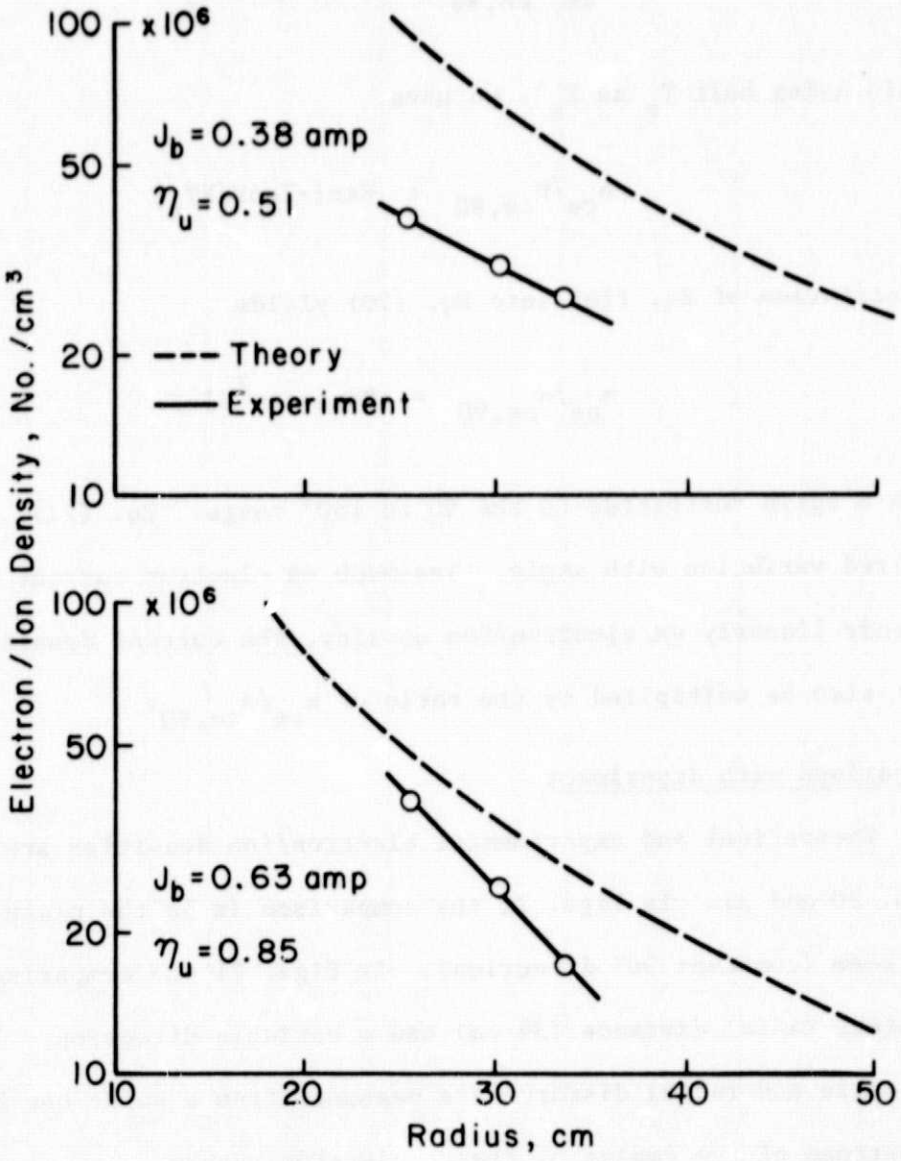

Fig. 20 - Comparison of Theoretical and Experimental Electron / Ion Densities Normal to Ion-beam. Axial Position is 7.5 cm Downstream of 15 cm Thruster.

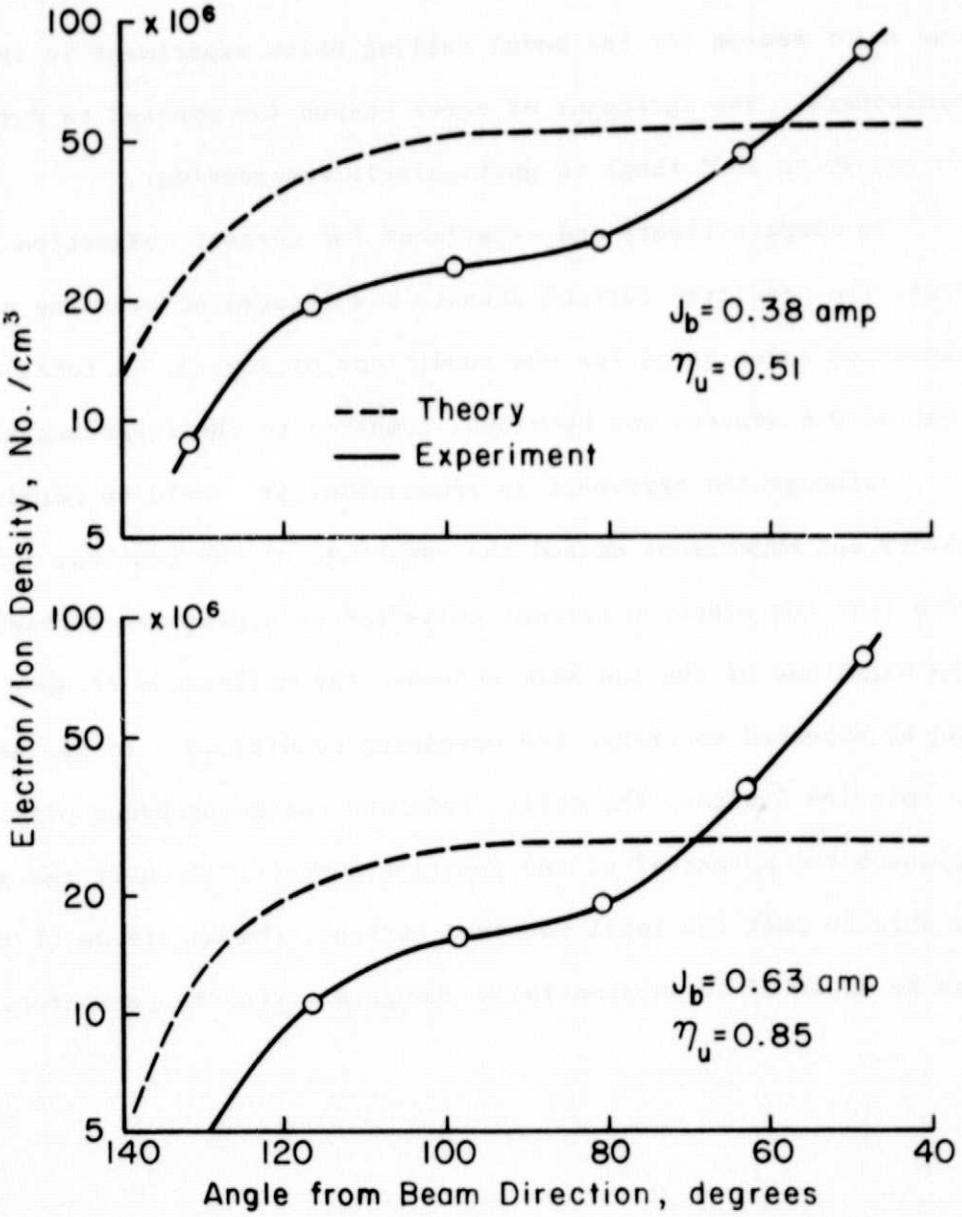

Fig. 21 - Comparison of Theoretical and Experimental Electron/Ion Densities at Radius of 34 cm from Axial Location 7.5 cm Downstream of 15 cm Thruster.

the radial or downstream direction. This initial bias is probably also the major reason for the model falling below experiment in the 90 to 180° hemisphere. The agreement of curve shapes (as opposed to curve levels) in the 90 to 180° range is particularly interesting.

To compare theory and experiment for current collection over a large area, the predicted current density was integrated over the area of the simulated solar array for the conditions of Fig. 5. A total electron current of 0.6 amperes was obtained, compared to the experimental value of 0.3.

Although the agreement is reasonable, it should be noted that both theory and experiment exceed the magnitude of the ion-beam current. Any time that the electron current collected on a positive surface approaches the magnitude of the ion beam current, the collection of such a current can be expected to change the operating conditions. If the neutralizer is emission limited, the entire beam and charge-exchange plasma will approach the potential of the positive surface. Even if the neutralizer is able to emit the total required current, the magnitude of the current can be expected to substantially change electron temperatures.

the radial or downstream direction. This initial bias is probably also the major reason for the model falling below experiment in the 90 to 180° hemisphere. The agreement of curve shapes (as opposed to curve levels) in the 90 to 180° range is particularly interesting.

To compare theory and experiment for current collection over a large area, the predicted current density was integrated over the area of the simulated solar array for the conditions of Fig. 5. A total electron current of 0.6 amperes was obtained, compared to the experimental value of 0.3.

Although the agreement is reasonable, it should be noted that both theory and experiment exceed the magnitude of the ion-beam current. Any time that the electron current collected on a positive surface approaches the magnitude of the ion beam current, the collection of such a current can be expected to change the operating conditions. If the neutralizer is emission limited, the entire beam and charge-exchange plasma will approach the potential of the positive surface. Even if the neutralizer is able to emit the total required current, the magnitude of the current can be expected to substantially change electron temperatures.

CONCLUDING REMARKS

Currents have been measured to positive-potential surfaces that are outside, but near, a thruster ion beam. These currents are primarily due to electron collection from the charge-exchange plasma that is generated by the ion beam and escaping neutral propellant. The barometric equation was found to approximately describe the potential-density variation in the charge-exchange plasma, although at an electron temperature about half that found in the ion beam.

Experimental data were obtained for several combinations of thruster operating conditions and geometry of nearby surfaces. Based upon the experimental data obtained, a simple model was derived for the charge-exchange plasma. This model is conservative in that both the electron/ion density and the electron current density should be equal to, or less than, the predicted value for all directions in the hemisphere upstream of the ion beam direction.

The model shows that increasing distance between a positive surface (such as a high-voltage solar array) and the thruster is the simplest way to control current collection. Other factors remaining unchanged, the collected current will vary inversely as the square of this thruster-surface distance. Moving a positive surface in the upstream direction will help, but the decrease will not be significant until the direction is 120 to 130° from the ion-beam direction. The downstream hemisphere should be avoided, if possible.

It should be noted that various techniques may be effective in reducing the charge-exchange plasma effects described herein. These techniques

include control of charge-exchange ions at their source, such as by trajectory deflection or collection of charge exchange ions. They also include control at the positive surface, such as electrostatic shielding of the positive surface or covering it with an insulating layer. Such techniques, though beyond the scope of the present investigation, may reduce the effects predicted herein.

REFERENCES

1. J. M. Sellen, Jr., W. Bernstein, and R. F. Kemp, Rev. Sci. Instr., Vol. 36, pp. 316-322 (1965).

2. H. S. Ogawa, R. K. Cole, and J. M. Sellen, Jr., AIAA Paper No. 69-263 (1969).

3. H. S. Ogawa, R. K. Cole, and J. M. Sellen, Jr., AIAA Paper No. 70-1142 (1970).

4. W. Knauer, J. R. Bayless, G. T. Todd, and J. W. Ward, NASA Contract Report CR-72675, May 1970.

5. G. K. Komatsu, R. K. Cole, D. K. Hoffmaster, and J. M. Sellen, Jr., AIAA Paper No. 75-428 (1975).

6. J. F. Staggs, W. P. Gula, and W. R. Kerslake, J. Spacecr. Rockets, Vol. 5, pp. 159-164 (1968).

7. R. Worlock, G. Trump, J. M. Sellen, Jr., and R. F. Kemp, AIAA Paper No. 73-1101 (1973).

8. G. Isaacson, in NASA Contract Report CR-134755 (by P. J. Wilbur), Appendix B, Dec. 1974.

9. F. F. Chen, "Plasma Diagnostic Techniques" (Huddelstone and Leonard, Eds.), Chapter 4, Academic Press, New York, 1965.

10. D. Bohm, in "The Characteristics of Electrical Discharges in Magnetic Fields" (A. Guthrie and R. K. Wakerling, Eds.), pp. 77-86, McGraw-Hill Book Co., 1949.

11. R. M. Kushnir, B. M. Palyukh, and L. A. sena, Bull. Acad. Sci. USSR, Phys. Ser., Vol. 23, pp. 995-999 (1959).

12. I. P. Iovitsu and N. Ionescu-Pallas, Sov. Phys. - Tech. Phys., Vol. 4, pp. 781-791 (1960).

13. D. Zuccaro, NASA Contract Report CR-72398 (1968).

14. L. L. Marino, A. C. H. Smith, and E. Caplinger, Phys. Rev., Vol. 128, pp. 2243-2250 (1962).

15. D. Rapp and W. E. Francis, J. Chem. Phys., Vol. 37, pp. 2631-2645 (1965).